



Effect of magnetic field on martensitic transition of Ni₄₆Mn₄₁In₁₃ Heusler alloy

著者	及川 勝成
journal or publication title	Applied Physics Letters
volume	88
number	12
page range	122507-1-122507-3
year	2006
URL	http://hdl.handle.net/10097/34936

Effect of magnetic field on martensitic transition of $\text{Ni}_{46}\text{Mn}_{41}\text{In}_{13}$ Heusler alloy

K. Oikawa,^{a)} W. Ito, Y. Imano, Y. Sutou, R. Kainuma, and K. Ishida

Department of Materials Science, Graduate School of Engineering, Tohoku University, 6-6-11 Aoba-yama, Sendai 980-8579, Japan

S. Okamoto and O. Kitakami

Institute of Multidisciplinary Research for Advanced Materials, Tohoku University, Katahira 2-1-1, Sendai 980-8577, Japan

T. Kanomata

Faculty of Engineering, Tohoku Gakuin University, 1-13-1 Chuo, Tagajo 980-8573, Japan

(Received 28 November 2005; accepted 30 January 2006; published online 21 March 2006)

Magnetic and martensitic transition behaviors of a $\text{Ni}_{46}\text{Mn}_{41}\text{In}_{13}$ Heusler alloy were investigated by differential scanning calorimetry and vibrating sample magnetometry. A unique martensitic transition from the ferromagnetic austenite phase to the antiferromagneticlike martensite phase was detected and magnetic-field-induced “reverse” transition was confirmed in a high magnetic field. In addition, a large positive magnetic entropy change, which reached 13 J/kg K at 9 T, was observed to accompany reverse martensitic transition. This alloy shows promise as a metamagnetic shape memory alloy with magnetic-field-induced shape memory effect and as a magnetocaloric material. © 2006 American Institute of Physics. [DOI: 10.1063/1.2187414]

Ferromagnetic shape memory alloys (FSMAs) have received much attention as high performance actuator materials, since the report of a large magnetic-field-induced strain by the rearrangement of twin variants in the martensite.¹ To date, several FSMAs, including Ni_2MnGa ,² Fe-Pd ,³ Fe-Pt ,⁴ Ni-Co-Ga ,^{5,6} Ni-Co-Al ,⁷ and Ni-Fe-Ga (Ref. 8) systems, have been reported. From the viewpoint of practical applications, magnetic-field-induced martensitic phase transition is more attractive than the rearrangement of martensite variants for a magnetically driven actuator because a larger output stress is expected. In Ni-Mn-Ga alloys, the shift of martensitic transition temperatures, such as the martensitic transition starting temperature M_s and the reverse transition finishing temperature A_f , with application of a magnetic field, are reported to be only 0.8–1.6 K under a field of 2 T, because the difference in magnetization ΔI between the martensite and austenite phases at the M_s and A_f is small due to the phase transition from the ferro- or paramagnetic austenite phase to the ferromagnetic martensite phase.⁹ This fact means that an extremely large magnetic field is required for magnetic-field-induced martensitic transition, in Ni-Mn-Ga alloys. In most other FSMAs, the situation is similar to that in the Ni-Mn-Ga alloys,^{2–8} namely, the magnetic-field-induced shape memory effect is difficult to obtain in the conventional FSMAs.

Very recently, the present author's group has found an unusual type of FSMAs showing the martensitic transition from the ferromagnetic austenite phase to the antiferro- or paramagnetic martensite phase in the Ni-Co-Mn-In Heusler alloy system and confirmed magnetic-field-induced reverse martensitic transition (MFIRT).¹⁰ An almost perfect shape memory effect associated with this phase transition is induced by a magnetic field and is called the metamagnetic shape memory effect.¹⁰ This alloy system opens up the pos-

sibility of utilizing the magnetic-induced shape memory effect. The Ni-Mn-In system is a basic ternary alloy system of the Ni-Co-Mn-In alloy. Experimental studies of the magnetic properties in this system have only focused on the stoichiometric composition the Ni_2MnIn alloy.^{11,12} The magnetic properties of the martensite phase and effect of a magnetic field on the martensitic transition have not as yet been reported, although the composition dependences of M_s and A_f and the Curie temperature T_c of the austenite phase in the $\text{Ni}_2\text{Mn}_{1+x}\text{In}_{1-x}$ alloys have been reported by Sutou *et al.*¹³ In the present study, the magnetic and martensitic transition behaviors of the $\text{Ni}_{46}\text{Mn}_{41}\text{In}_{13}$ alloy, which was selected as a sample with a relatively high T_c and large ΔI ,¹⁴ were investigated, and the MFIRT from an antiferromagneticlike martensite phase to a ferromagnetic austenite phase was confirmed.

A $\text{Ni}_{46}\text{Mn}_{41}\text{In}_{13}$ alloy weighing about 20 g was prepared by induction melting under an argon gas atmosphere. The obtained ingots were cut into small pieces by a diamond saw and homogenized at 1173 K for 24 h in a vacuum and then quenched in ice water. The martensitic transition temperature was determined by differential scanning calorimetry (DSC) at heating and cooling rates of 10 K/min, and the magnetic properties were determined by vibrating sample magnetometry and a sample extraction method at heating and cooling rates of 3 K/min. The T_c was defined as the minimum point of temperature derivative of magnetization under a field strength H of 0.05 T. Transmission electron microscopic observation and x-ray diffraction (XRD) of powder specimens were conducted to identify the crystal structure of both austenite and martensite phases.

The selected area diffraction (SAD) patterns of the austenite and martensite phase of the $\text{Ni}_{46}\text{Mn}_{41}\text{In}_{13}$ alloy are shown in Fig. 1. For the austenite phase, $\{111\}_{L21}$ ordered spots, characterized as the $L2_1$ structure, can be clearly observed as shown in Fig. 1(a). In addition, the lattice constant of the $L2_1$ structure was evaluated as $a=0.60163$ nm from

^{a)}Electronic mail: k-oikawa@material.tohoku.ac.jp

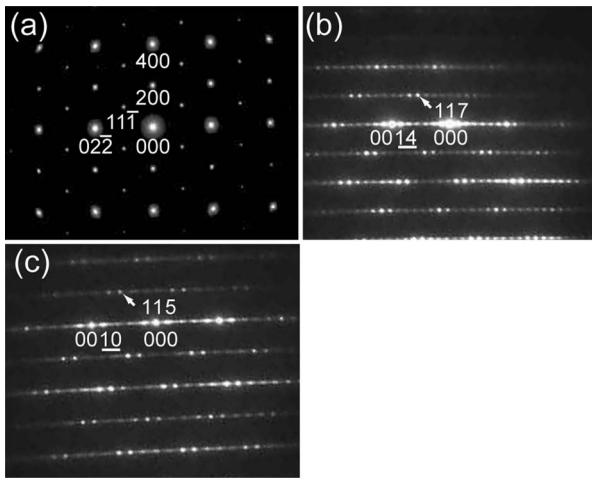


FIG. 1. SAD patterns taken from (a) austenite phase at room temperature, and (b) and (c) martensite phase at 83 K in the $\text{Ni}_{46}\text{Mn}_{41}\text{In}_{13}$ alloy.

the XRD pattern. For the martensite phase, $x/7\{220\}_{\text{L21}}$ and $x/5\{220\}_{\text{L21}}$ extra reflections are observed as shown in Figs. 1(b) and 1(c), respectively. Thus, the martensite phase consists of a mixture of 14 M and 10 M structures, which was also confirmed by the XRD pattern.

The thermomagnetization curves of the $\text{Ni}_{48}\text{Mn}_{41}\text{In}_{13}$ alloy under magnetic field strengths of 0.05, 2, and 7 T are shown in Fig. 2. The magnetization slightly decreases with increasing temperature in the low-temperature region and significantly rises around 223 K under a field strength of 0.05 T. Since the martensitic transition temperatures determined by DSC are $M_s=234$ K, $M_f=204$ K, $A_s=222$ K, and $A_f=255$ K, where the M_f and A_s are the martensitic transition finishing and reverse transition starting temperatures, respectively, the increase of magnetization at around 223 K can be explained as being due to the reverse martensitic transition. In the austenite phase region, the magnetization drastically decreases in the vicinity of the T_c of 296 K after a steady stage. The thermal hysteresis of the thermomagnetization curves is significantly small.

Such a behavior in a low magnetic field, which shows a step due to martensitic transition in the magnetization curve, has also been reported in conventional FSMA. ²⁻⁸ The origin of this magnetization jump of the conventional FSMA in the low magnetic field is a large magnetic anisotropy energy difference between a martensite and an austenite phase, and the magnetization jump vanishes or changes in a slightly high magnetic field. ²⁻⁸ In the $\text{Ni}_{48}\text{Mn}_{41}\text{In}_{13}$ alloy, however, a

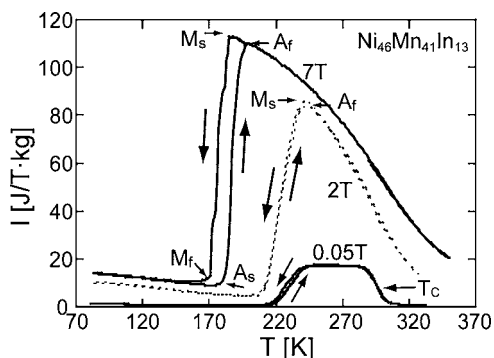


FIG. 2. Thermomagnetization curves of the $\text{Ni}_{46}\text{Mn}_{41}\text{In}_{13}$ alloy under various magnetic fields.

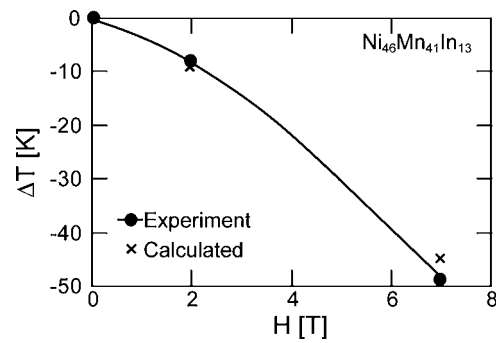


FIG. 3. Magnetic field dependence of the A_f temperature change in the $\text{Ni}_{46}\text{Mn}_{41}\text{In}_{13}$ alloy.

large magnetization jump associated with the martensitic transition temperature is still observed in high magnetic fields of 2 and 7 T as shown in Fig. 2. This result suggests that the magnetic spin is reorientated during the martensitic transition. The martensitic transition temperatures obviously decrease with increasing magnetic field. The thermal hysteresis of the martensitic transition under the field of 7 T is larger than those under lower magnetic fields. The reason for this change is not clear at present. A large difference in magnetization, ΔI , between the austenite and martensite phases is preferred to obtain a large martensitic temperature shift, ΔT , induced by a magnetic field. ¹⁰ Values of ΔT determined from the magnetization curves shown in Fig. 2 are plotted in Fig. 3. The difference in martensitic transition temperature between 0.05 T and 7 T is $\Delta T=224.1$ K. The ΔT induced by magnetic field change ΔH is approximately given by the Clausius–Clapeyron relation in the magnetic phase diagram,

$$\Delta T \approx \left(\frac{\Delta I}{\Delta S} \right) \Delta H, \quad (1)$$

where ΔI and ΔS are the differences in magnetization and entropy between the austenite and martensite phases, respectively. The ΔS of the $\text{Ni}_{48}\text{Mn}_{41}\text{In}_{13}$ alloy is calculated from the enthalpy data obtained by the DSC as 17.1 J/K kg. Theoretical values of ΔT calculated from Eq. (1) using ΔH and ΔI shown in Fig. 2 are plotted with the experimental data in Fig. 3, where the agreement between experimental and theoretical values is quite satisfactory.

Magnetization curves of the $\text{Ni}_{48}\text{Mn}_{41}\text{In}_{13}$ alloy at various temperatures are shown in Fig. 4(a). The measurement was conducted by heating from 100 K to 273 K. The magnetization curve in the martensite phase at 100 K is slightly convex, while that in the austenite phase at 273 K shows typical ferromagnetic behavior. The Arrott plot of the magnetization curve of the martensite phase is shown in Fig. 4(b). $I^2 \approx 0$ is obtained by extrapolation in $H/I \rightarrow 0$ from the high magnetic field, namely, the spontaneous magnetization is zero in the martensite phase. In addition, the temperature dependence on the magnetic susceptibility $\chi_{0.05 \text{ T}}$ of the martensite phase taken from zero-field-cooled (ZFC) and field-cooled (FC) specimens are shown in Fig. 4(c), where a magnetic field of 0.05 T was applied for the FC specimen. The $\chi_{0.05 \text{ T}}$ of the ZFC shows a maximum although the $\chi_{0.05 \text{ T}}$ of the FC monotonously decreases with increasing temperature. These facts suggest that the martensite phase is magnetically inhomogeneous.

It is interesting to note that the curves at 180 and 200 K show a metamagnetic phase transition from the antiferro-

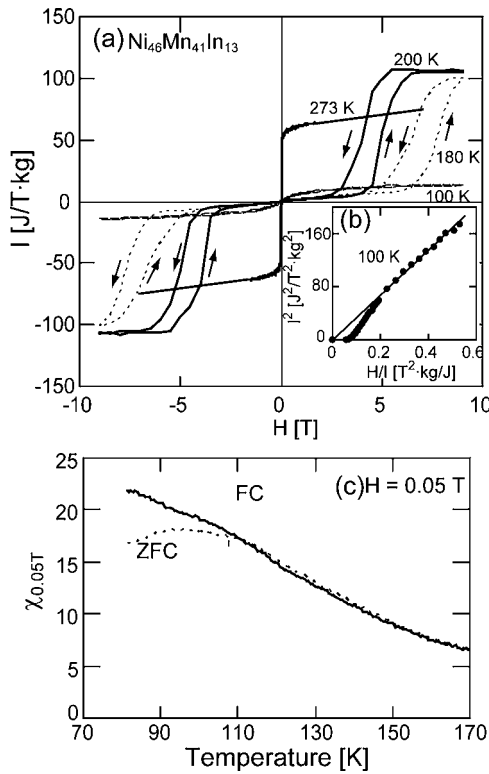


FIG. 4. (a) Magnetization curves of the $\text{Ni}_{46}\text{Mn}_{41}\text{In}_{13}$ alloy at various temperatures, (b) Arrot plot curves at 100 K, and (c) temperature dependence of magnetic susceptibility of martensite phase under a magnetic field of 0.05 T.

magneticlike martensite phase to the ferromagnetic austenite phase, which is in accordance with the thermomagnetization behavior shown in Fig. 2. This magnetic behavior is similar to that in NiCoMnIn alloys,¹⁰ and the metamagnetic shape memory effect is also expected in this alloy. In addition, a large magnetic-field-induced entropy change, ΔS_m , is expected from the magnetization curves. The ΔS_m can be obtained from the magnetization curves using the Maxwell relation:

$$\Delta S_m = \int_0^H \left(\frac{\partial I}{\partial T} \right) dH. \quad (2)$$

The equation of the numerically integrating Eq. (2) using a trapezoidal rule can be described as follows:

$$\Delta S_m(T_{av})_{\Delta H} \approx \frac{\Delta H}{2\Delta T} \left(\Delta I_1 + 2 \sum_{k=2}^{n-1} \Delta I_k + \Delta I_n \right). \quad (3)$$

Here, T_{av} and ΔT are the average temperature and temperature difference of two isothermal magnetization curves, respectively, ΔH is the changing step of the applied magnetic field, and ΔI_k is the difference of the magnetization at the magnetic field $k \times \Delta H$ between the two isothermal magnetization curves, where k is the step number of the applied magnetic field, and $k=1$ and $k=n$ are corresponding to the first step as $H=0$ and the last step as the maximal applied field, respectively. The ΔS_m value at 190 K for an average temperature from two magnetization curves at 180 and 200 K in Fig. 4(a) are calculated by Eq. (3) and plotted in

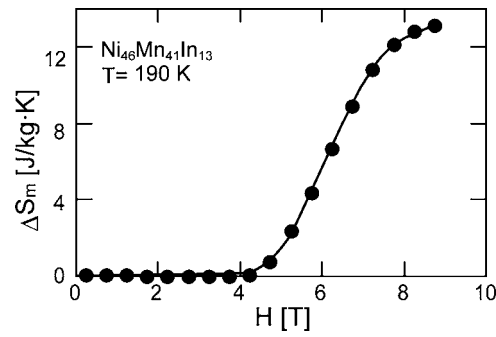


FIG. 5. Magnetic-field-induced entropy change, ΔS_m , of the $\text{Ni}_{46}\text{Mn}_{41}\text{In}_{13}$ alloy.

Fig. 5, where the ΔT and ΔH are 20 K and 0.5 T, respectively. The maximum value of ΔS_m reaches 13 J/K kg, which is comparable with other magnetocaloric materials, such as the $\text{Gd}_5\text{Si}_2\text{Ge}_2$ alloy.¹⁵ This high value of ΔS_m suggests that this alloy system is promising as a candidate for magnetocaloric materials.

In conclusion, magnetic and martensitic transition behaviors of $\text{Ni}_{46}\text{Mn}_{41}\text{In}_{13}$ Heusler alloys were investigated, and martensitic transition associated with metamagnetic transition was observed in this alloy system from the antiferromagneticlike martensite phase to the ferromagnetic austenite phase. The magnetic-field-induced reverse martensitic transition was experimentally confirmed. Consequently, this alloy system shows promise for use as metamagnetic shape memory materials as well as magnetocaloric materials.

The present study was supported by a Grant-in-Aid from CREST, Japan Science and Technology Agency and a “Collaborative Research” grant from the Center for Interdisciplinary Research, Tohoku University.

¹K. Ullakko, J. K. Huang, C. Kanter, V. V. Kokorin, and R. C. O’Handley, *Appl. Phys. Lett.* **69**, 1966 (1996).

²P. J. Webster, K. R. A. Ziebeck, S. L. Town, and M. S. Peak, *Philos. Mag. B* **49**, 295 (1984).

³R. D. James and M. Wuttig, *Philos. Mag. A* **77**, 1273 (1998).

⁴T. Kakeshita, T. Takeuchi, T. Fukuda, T. Saburi, R. Oshima, S. Muto, and K. Kishio, *Mater. Trans., JIM* **41**, 882 (2000).

⁵M. Wuttig, J. Li, and C. Craciunescu, *Scr. Mater.* **44**, 2393 (2001).

⁶K. Oikawa, T. Ota, F. Gejima, T. Ohmori, R. Kainuma, and K. Ishida, *Mater. Trans., JIM* **42**, 2472 (2001).

⁷K. Oikawa, L. Wulff, T. Iijima, F. Gejima, T. Ohmori, A. Fujita, K. Fukamichi, R. Kainuma, and K. Ishida, *Appl. Phys. Lett.* **79**, 3290 (2001).

⁸K. Oikawa, T. Ota, T. Ohmori, Y. Tanaka, H. Morito, A. Fujita, R. Kainuma, K. Fukamichi, and K. Ishida, *Appl. Phys. Lett.* **81**, 5201 (2002).

⁹V. V. Khovailo, N. Novosad, T. Takagi, D. A. Filippov, R. Z. Levitin, and A. N. Vasil’ev, *Phys. Rev. B* **70**, 174413 (2004).

¹⁰R. Kainuma, Y. Imano, W. Ito, Y. Sutou, H. Morito, S. Okamoto, O. Kitakami, K. Oikawa, A. Fujita, T. Kanomata, and K. Ishida, *Nature (London)* **439**, 957 (2006).

¹¹M. B. Stearns, *J. Appl. Phys.* **50**, 2060 (1979).

¹²T. Kanomata, K. Shirakawa, and T. Kaneko, *J. Magn. Magn. Mater.* **65**, 76 (1987).

¹³Y. Sutou, Y. Imano, N. Koeda, T. Omori, R. Kainuma, K. Ishida, and K. Oikawa, *Appl. Phys. Lett.* **85**, 4358 (2004).

¹⁴W. Ito, Y. Imano, Y. Sutou, K. Oikawa, R. Kainuma, and K. Ishida (unpublished).

¹⁵V. K. Pecharsky and K. A. Gschneidner Jr., *Phys. Rev. Lett.* **78**, 4494 (1997).